WATER TUNNEL RESULTS OF LEADING-EDGE VORTEX FLAP TESTS ON A DELTA WING VEHICLE

John H. Del Frate
NASA Ames Research Center
Dryden Flight Research Facility
Edwards, California

SUMMARY

A water tunnel flow visualization test on leading-edge vortex flaps was conducted at the flow visualization facility of the NASA Ames Research Center's Dryden Flight Research Facility. The purpose of the test was to visually examine the vortex structures caused by various leading-edge vortex flaps on the delta wing of an F-106 model. The vortex flaps tested were designed analytically and empirically at the NASA Langley Research Center. The three flap designs were designated as full-span gothic flap, full-span untapered flap, and part-span flap.

The test was conducted at a Reynolds number of 76,000/m (25,000/ft). This low Reynolds number was used because of the 0.076-m/s (0.25-ft/s) test section flow speed necessary for high-quality flow visualization. However, this low Reynolds number may have influenced the results.

Of the three vortex flaps tested, the part-span flap produced what appeared to be the strongest vortex structure over the flap area. The full-span gothic flap provided the next best performance.

INTRODUCTION

The vortex flap concept was conceived under the assumption that if the flap can be designed through planform shaping and/or twist to promote vortex flow reattachment along the hinge line at design lift, pressure distributions that reduce drag most efficiently per unit flap area will be established on the flap.[1] For a vortex flap to perform optimally, it should capture the entire leading-edge vortex on its upper surface and provide flow reattachment on the upper surface leading edge at or near the hinge line.[2]

To evaluate this concept, four vortex flaps were designed for the F-106 model. Three of these are bolt-on types and one is an integral type. The bolt-on flaps extend from the underside and ahead of the wing leading edge; integral flaps, when undeflected, are a part of the wing planform. The three bolt-on flaps, shown in figure 1,* include an analytically designed full-span gothic flap, an untapered empirical variation of the full-span gothic flap, and an analytically designed

*Color prints of figures 2, 5, 6, and 7 are available from the author.

part-span flap. The bolt-on flaps were designed for a Mach number of 0.3 and 30° downward deflection. The integral flap was designed for a Mach number of 0.8 and 40° downward deflection.

These flaps have been extensively tested in various wind tunnels on different scale models and at different Reynolds numbers. To better understand the vortex structure, Langley and Ames-Dryden jointly conducted a test on the three bolt-on flap configurations using an F-106A model. (An F-106A model was used instead of the F-106B model because of availability. Only slight geometric differences exist between the models, and these occur in locations that should not affect the flow field in the regions of interest.)

EXPERIMENTAL METHODS

Water Tunnel Facility

Except for a few modifications, the Ames-Dryden flow visualization facility (FVF) is based on the design of the Northrop Corporation closed-return water tunnel. Figure 2 shows a schematic of the FVF. The test section measures 0.41 m by 0.61 m (16 in. by 24 in.) and is 1.83 m (72 in.) long. The test section is oriented vertically and is made entirely of 5.08-cm (2-in.) thick plexiglass, which allows for 360° viewing of the tests. There is a door on the side of the test section for convenient access to the model and the support mechanism.

In general, the model angle of attack can be remotely varied ±45°, and the sideslip angle can be varied ±15° between runs. The velocity range of the FVF can be varied from 0.013 m/s (0.04 ft/s) to 0.335 m/s (1.1 ft/s). The flow velocity of the test section for this test was 0.076 m/s (0.25 ft/s), which is equivalent to a Reynolds number of 76,000/m (23,000/ft). This velocity is typically used because it allows excellent flow visualization.

The visualization technique used in this test is the colored dye technique. With this technique, colored dyes are pumped into the flow field through dye lines to provide a three-dimensional view of the flow.

Model Description

The model tested was a modified 1/48-scale F-106A hobby model (figure 3). The modifications included the following:

1. The landing gear was placed in the retracted position

2. The inlets were made operational in order to simulate the proper mass flow ratio

3. The ailerons were repositioned to a zero deflection; the model originally came with the ailerons in the down position

4. Eight dye lines were installed externally underneath the wing with aluminum tape. The eight dye ports were located along the leading edge of the vortex flap (figure 2). Dye port locations were determined by trial and error.

5. Three different vortex flaps were installed on the model. Each vortex flap was tested with various deflection angles (see table 1). The flaps were formed from aluminum and bent to the proper deflection angle, and their leading edges were sharpened. These flaps were then attached to the underside of the wing with double-sided tape (figure 4).

Test Procedure

Each configuration was tested at sideslip $\beta = 0°$ and at 8°, 10°, 12°, 14°, 16°, and 20° angles of attack. Some configurations were also tested at a 6° angle of attack. In addition, most of the configurations were tested at $\beta = +5°$.

The colored dye flow visualization technique was used because the primary purpose of this experiment was to provide localized three-dimensional views of any vortical activity on or near the vortex flaps. This technique allowed visualization of the vortex structure developed by the vortex flaps.

Data were recorded visually using both videotape and 35-mm slide film. Slides were taken of both the side view and the plan view of the model at sideslip $\beta = 0°$. At $\beta = +5°$, slides were taken of only the plan view. Videotape records were taken of only the plan view. Notes on peculiarities, trends, and onsets were recorded for each test run.

RESULTS AND DISCUSSION

This discussion is limited to a few selected cases. These cases illustrate general trends and are representative of the various configurations tested.

Performance Criteria

In a water tunnel flow visualization test, one is usually limited to a strictly qualitative set of data recorded at a very low Reynolds number. This was considered acceptable for the vortex flap test. As a result, performance criteria were limited to

1. strength of the leading-edge vortex that develops on the vortex flap (that is, vortex definition, rotation rate, length, and stability)

2. leading-edge vortex persistence (that is, the range of angle of attack through which the leading-edge vortex exists)

General Introductory Comments for All Configurations

$\beta = 0°$. — In general, all flap configurations exhibit the same behavior at angles of attack α in the range $0° \leqslant \alpha \leqslant 8°$. In this range, the flow on the upper surface of the flap and the wing is attached and laminar. As the angle of attack increases above a certain value ($8° \leqslant \alpha \leqslant 14°$, depending on the configuration) the flow on the upper surface of the flap begins to separate. As the flow separates, the leading-edge vortex begins to develop. As the angle of attack is increased, the leading-edge vortex continues to grow in strength.

With some configurations, as the leading-edge vortex develops there is a continuous shedding of this vortex at a consistent frequency. The leading-edge vortex is formed, then the whole vortex sheds itself from the flap and proceeds parallel (for the most part) to the flap over the upper wing surface. As this is taking place another leading-edge vortex has developed on the upper surface of the vortex flap. In addition, as the vortex gains strength, the portion of the leading-edge vortex towards the rear of the flap starts to lift off the flap surface, and separated stagnant backflow starts to creep forward along the surface of the vortex flap. The extent of this type of flow varies with each configuration.

$\beta = +5°$. — In general, the same trends noted for the $\beta = 0°$ case pertain to the $\beta = +5°$ case. The main difference is that the onset of any particular flow condition occurs at an angle of attack approximately 2° lower on the leeward flap and approximately 2° higher on the windward flap than in the $\beta = 0°$ case.

Full-Span Gothic Vortex Flap

$\beta = 0°$. — With all configurations tested, the angle of attack at which the leading-edge vortex forms on the surface of the vortex flap is a function of the flap deflection angle. For the full-span gothic flap, approximate angles for the onset of vortex development are as follows:

Flap deflection δ, deg	Angle of attack α for vortex formation, deg
30	9
40	9
50	10
60	12

Results for 30° flap deflection, shown in figure 5, are discussed here. At $\alpha = 9°$, a leading-edge vortex develops that is immediately shed. As the leading-edge vortex sheds from the vortex flap it travels past the hinge line to merge with two vortices on the wing surface. The forward section (approximately 30 to 40 percent of the leading-edge vortex) of the shed vortex merges with a vortex that originates at the forward wing/fuselage juncture (from this point on, this vortex will be referred to as the juncture vortex). The juncture vortex lies farther inboard and is approximately parallel to the fuselage. The remainder of the shed vortex travels just past the hinge line to merge with a vortex that lies approximately parallel to the hinge line (from this point on, this vortex will be referred to as the hinge line vortex). As the angle of attack increases ($\alpha > 9°$) the leading-edge vortices pro-

duced by the vortex flap increase in strength. As these vortices shed, they tend to increasingly feed the hinge line vortex, making it stronger, until it eventually overcomes and merges with the juncture vortex, becoming the only vortex structure seen on the surface of the wing. This occurs at $\alpha \cong 18°$. At the upper angle-of-attack test limit of 20°, results remain approximately the same.

$\beta = +5°$. — The results noted previously in the general introductory comments also apply to the $\beta = +5°$ case.

Performance. — Based on the performance criteria, the full-span gothic flap produces a strong leading-edge vortex. The leading-edge vortex existed from $\alpha \cong 9°$ on up past 20° at what was judged to be the optimum flap deflection ($\delta = 30°$).

Full-Span Untapered Vortex Flap

$\beta = 0°$. — The results for the full-span untapered flap varied significantly from those of the other two flaps tested.

Again, the angle of attack at which the leading-edge vortex develops on the flaps varies with the deflection angle. For the full-span untapered flap, the approximate onset angles are as follows:

Flap deflection δ, deg	Angle of attack α for vortex formation, deg
30	8
40	10
40[a]	12
50	12

[a]Hinge gap filled in with modeling clay.

Results for the 50° flap deflection, shown in figure 6, are discussed here. At $\alpha = 12°$, a leading-edge vortex develops and is shed immediately (as described previously in the section concerning comments for all configurations). The vortex is different than those produced by the other flaps in that once the vortex is shed onto the wing upper surface it moves across and off the wing surface at the trailing edge of the wing.

The full-span untapered flap continues to develop leading-edge vortices at angles of attack up to 20° (and greater at some deflections); however, at $\alpha = 20°$ the strength of the juncture vortex overcomes everything else on the upper surface of the wing, and details are not well visualized.

It was thought that the discontinuity of the juncture between the flap surface and the wing leading edge might be the cause of the vortex shedding. Therefore, modeling clay was applied to smooth out the discontinuity. The modeling clay was applied such that the leading edge of the flap and the leading edge of the wing would form the edges of a smooth plane. After this modification, the leading-edge vortex continued to shed, and performance change, if any, was negative.

It was then hypothesized that the vortex shedding might be a Reynolds number effect instead of a configuration effect. At a Reynolds number this low, one might expect flow reattachment failure at the hinge line.[3] This in turn may be another

explanation as to why the leading-edge vortex is shed instead of remaining on the vortex flap.

$\beta = +5°$. – The results noted previously in the general introductory comments also apply to the $\beta = +5°$ case.

Performance. – The leading-edge vortex formed on the full-span untapered flap appears to have good definition. However, it is not as strong as that exhibited by the gothic flap. A flap deflection of 50° was judged to be the best for the full-span untapered vortex flap.

Part-Span Untapered Vortex Flap

$\beta = 0°$. – For the part-span untapered flap, the angles of attack at which the leading-edge vortex develops on the surface of the vortex flap are as follows:

Flap deflection δ, deg	Angle of attack α for vortex formation, deg
30	10
40	10
50	12
60	14

Results for the 30° flap deflection, shown in figure 7, are discussed here. At $\alpha = 10°$, a leading-edge vortex develops on the flap surface and immediately sheds onto the upper surface of the wing. At $\alpha \cong 12°$, the hinge line vortex (similar to the one observed on the Gothic flap) appears and merges with the shed leading-edge vortices. As the angle of attack increases to 14°, the forward 30 to 40 percent of the leading-edge vortex no longer sheds. It is stationary and very strong on the upper surface of the flap. At $\alpha \cong 20°$, the rear section of the leading-edge vortex stops shedding, and it no longer develops on the flap surface but rather on the wing. The leading-edge vortex starts at the forward end of the flap and travels along approximately 30 to 40 percent of the flap where it turns streamwise until it goes off the trailing edge of the wing.

All the part-span flap configurations develop a leading-edge vortex beyond $\alpha = 20°$.

Though not shown herein, the part-span flap at 60° deflection did not follow the general behavior of the other flap configurations; it never developed the hinge line vortex like the others did. This configuration allowed a strong juncture vortex to exist throughout all angles of attack tested. At $\alpha \geq 14°$ the flow coming over the flap surface separated, and the flap began producing leading-edge vortices that merged with the juncture vortex. This trend continued at $\alpha > 20°$.

$\beta = +5°$. – The results noted previously in the general introductory comments also apply to the $\beta = +5°$ case.

Performance. – The part-span vortex flap performed very well (compared with the other flaps) with respect to its ability to hold a leading-edge vortex on the surface of the flap. Although this flap did not maintain a leading-edge vortex along

the full length of the flap, its performance was better than that of the other flaps. The strength and stability of the leading-edge vortex produced by the part-span vortex flap were judged to be the strongest of those observed. A part-span vortex flap deflection of 30° proved to be the best of the part-span flap configurations.

CONCLUSIONS

Of the three sets of flap configurations tested, the part-span vortex flap at 30° deflection was judged to be the most effective leading-edge vortex flap based on the performance criteria used. The full-span gothic vortex flap at 30° deflection was the next most effective.

The low Reynolds number of 76,000/m (25,000/ft) may have been the cause for the flow failing to reattach after having traveled over the vortex structure on the flap. This in turn may have caused the periodic shedding of the leading-edge vortex.

Each of the three sets of vortex flap configurations changed the wing flow field significantly.

REFERENCES

1. Frink, Neal T.: Concept for Designing Vortex Flap Geometries (U). NASA TP-2233, 1983.

2. Ghaffari, Farhad, and Lamar, John E.: An Attached Flow Design of a Non-interfering Leading Edge Extension to a Thick Delta Wing. AIAA Paper 85-0350, 1985.

3. Carmichael, B.H.: Low Reynolds Number Airfoil Survey, Vol. 1. NASA CR-165803, 1981.

TABLE 1. — LEADING-EDGE VORTEX FLAP TEST CONDITIONS[a]

Full-span gothic flap		Full-span untapered flap		Part-span flap	
δ, deg	β, deg	δ, deg	β, deg	δ, deg	β, deg
30	0	30	0	30	0
30	5	40	0	30	5
40	0	40[b]	0	40	0
40	5	40	5	40	5
50	0	50	0	50	0
50	5	50	5	50	5
60	0			60	0
60	5			60	5

[a]Angle-of-attack range varied from 6° to 20°.

[b]Hinge gap filled in with modeling clay.

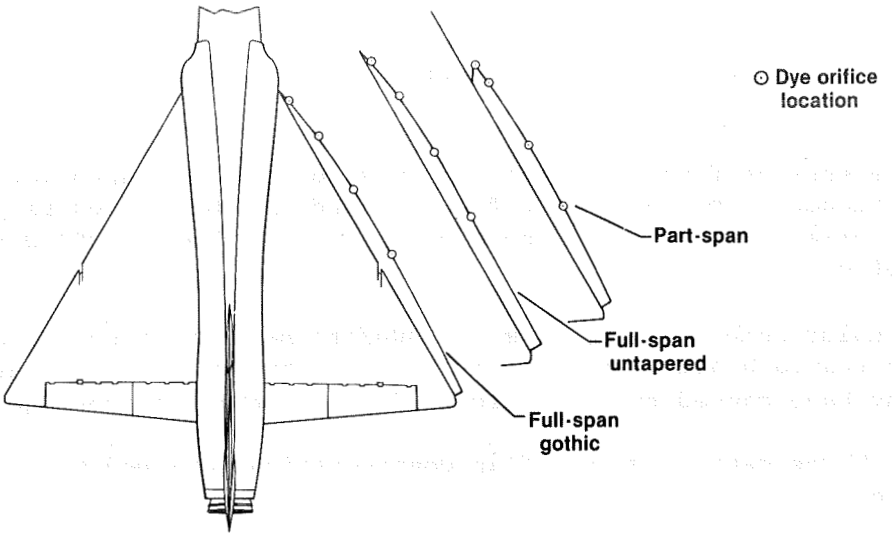

Figure 1. Schematic of flap planforms and dye orifice locations.

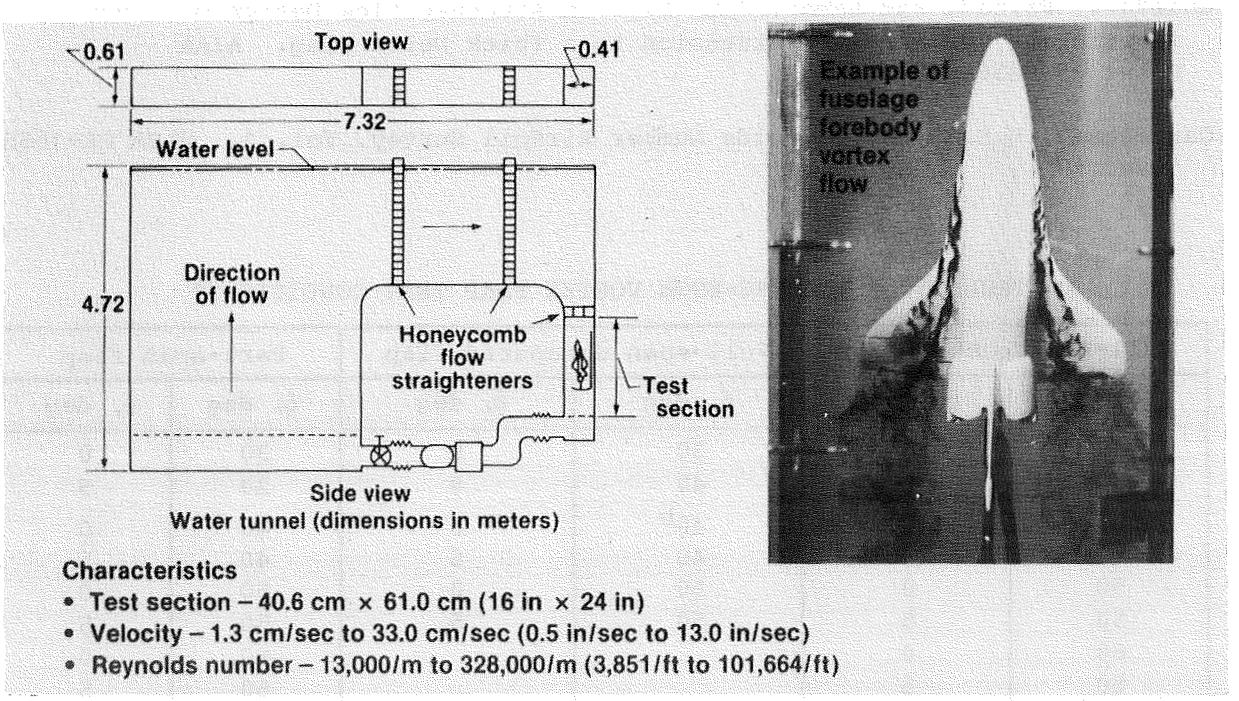

Figure 2. Flow visualization facility schematic and photograph of model in test section.

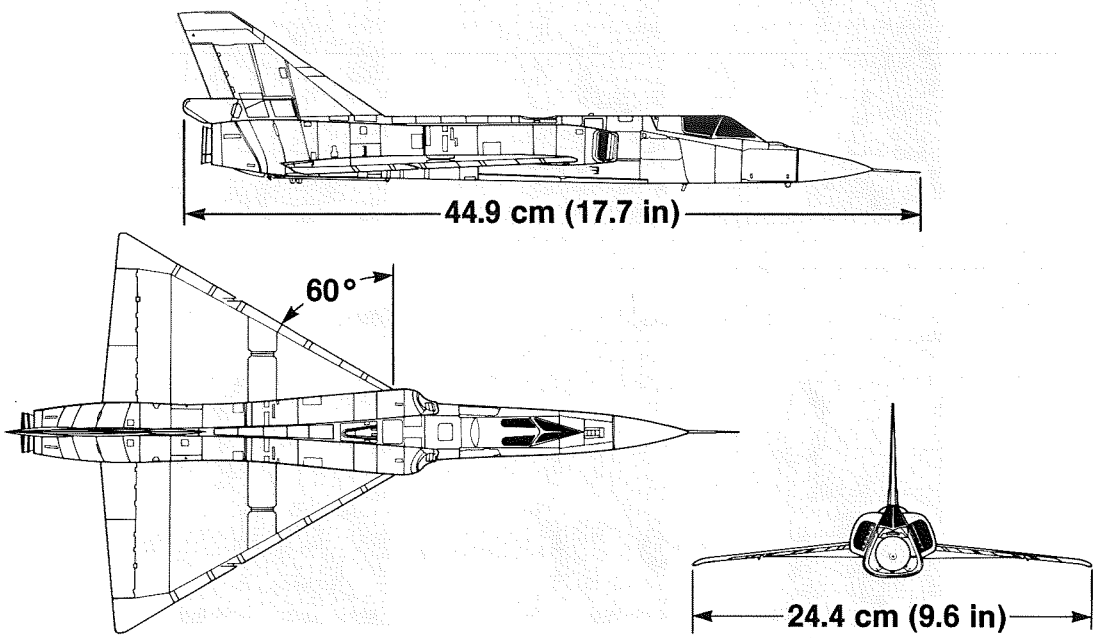

Figure 3. Three-view drawing of F-106A model with overall dimensions.

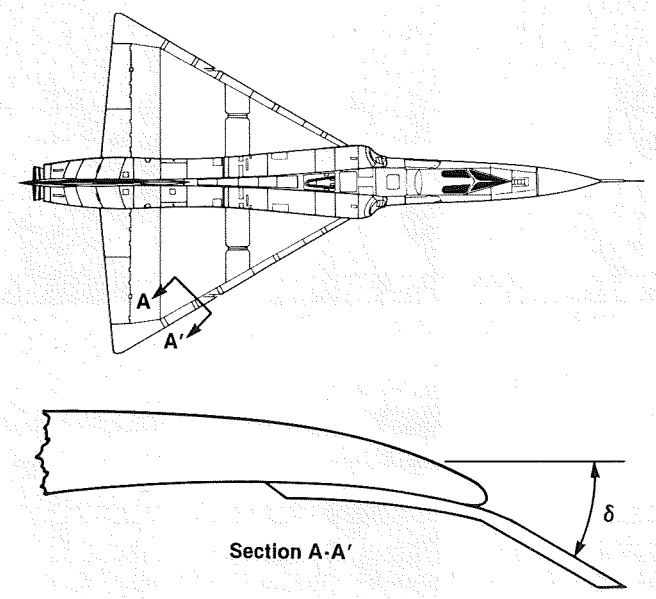

Figure 4. Typical cross-sectional view of an F-106 wing leading edge and a bolt-on flap.

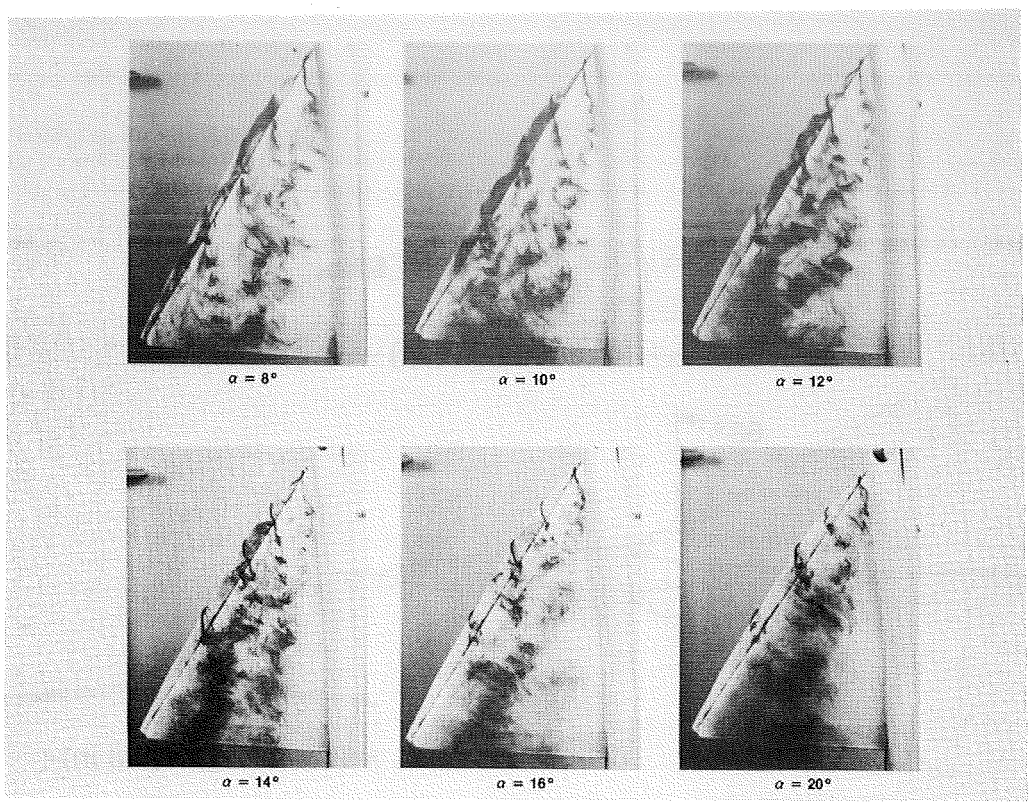

Figure 5. Results from the full-span gothic vortex flap test with flap deflected 30° (top view, left wing).

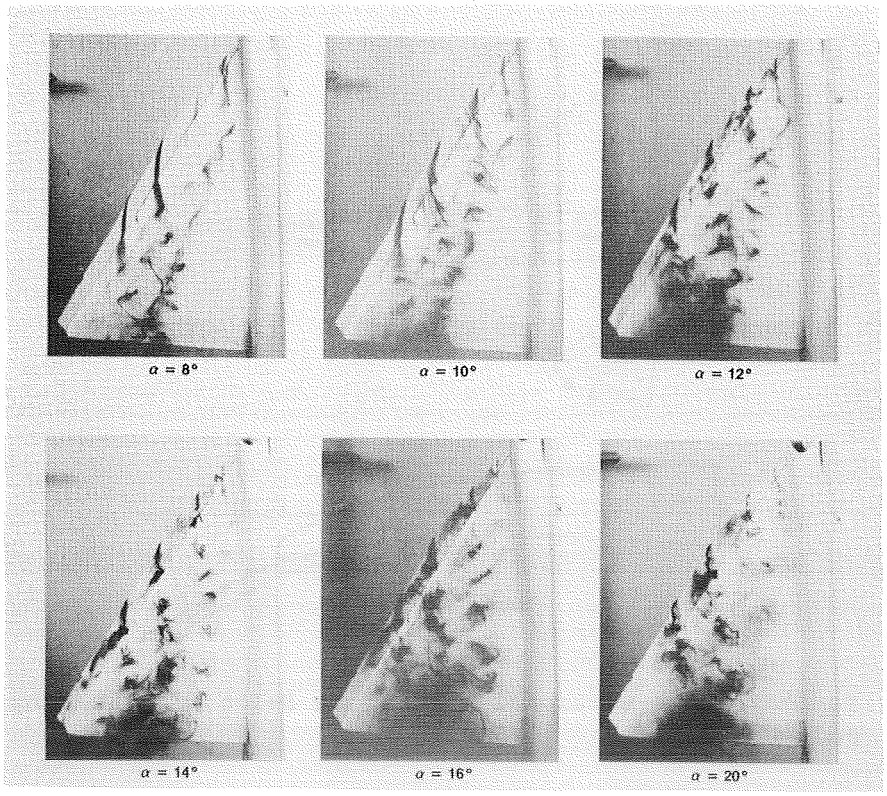

Figure 6. Results from the full-span untapered vortex flap test with flap deflected 50° (top view, left wing).

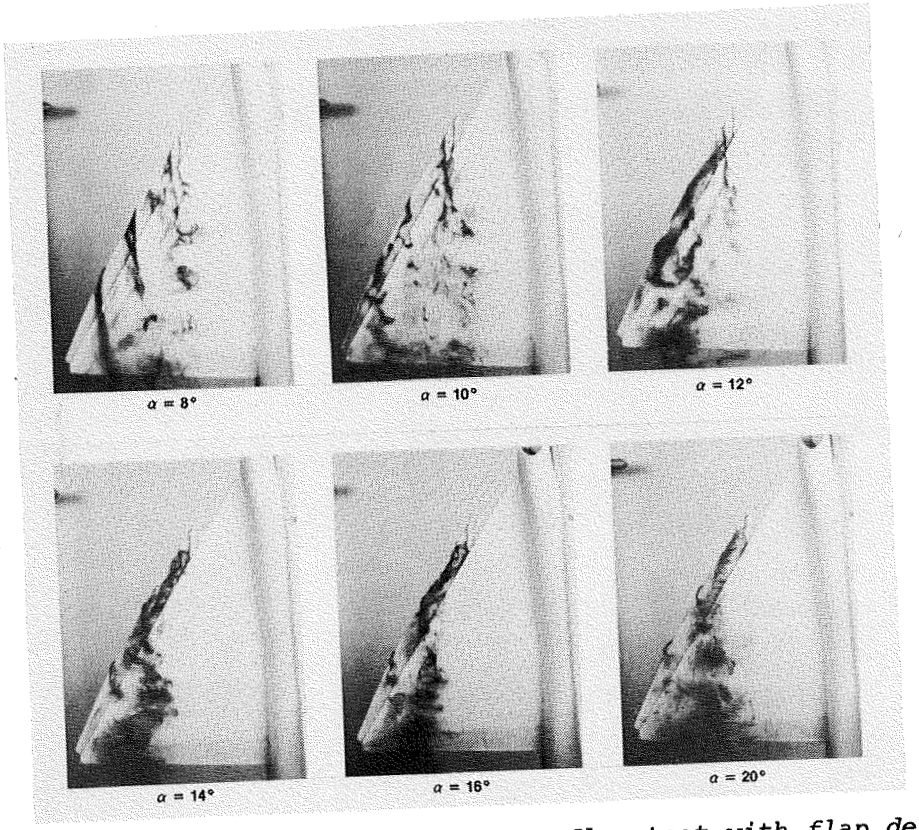

Figure 7. Results from the part-span vortex flap test with flap deflected 30° (top view, left wing).